BARC-1502

BARC-1502

STUDIES ON FOURIER AMPLITUDE SPECTRA OF ACCELEROGRAMS RECORDED ON ROCK SITES

by

A . K. Ghosh and K. S. Rao
Reactor Analysis and Systems Division

1990

BIBLIOGRAPHIC DESCRIPTION SHEET FOR TECHNICAL REPORT
(as per IS : 9400 - 1980)

01	*Security classification*	Unclassified
02	*Distribution :*	External
03	*Report status*	New
04	*Series :*	B.A.R.C. External
05	*Report type :*	Technical Report
06	*Report No. :*	B.A.R.C.-1502
07	*Part No. or Volume No. :*	
08	*Contract No. :*	
10	*Title and subtitle :*	Studies on Fourier amplitude spectra of accelerograms recorded on rock sites
11	*Collation :*	11 p., 19 figs., 1 tab., 1 appendix (p. A.1-A.2)
13	*Project No. :*	
20	*Personal author(s) :*	A.K. Ghosh; K.S. Rao
21	*Affiliation of author(s) :*	Reactor Analysis and Systems Division, Bhabha Atomic Research Centre, Bombay
22	*Corporate author(s) :*	Bhabha Atomic Research Centre, Bombay
23	*Originating unit :*	Reactor Analysis and Systems Division, B.A.R.C.
24	*Sponsor(s) Name :*	Department of Atomic Energy
	Type :	Government

Contd. ...(ii)

30	***Date of submission :***	February 1990
31	***Publication/Issue date :***	March 1990
40	***Publisher/Distributor :***	Bhabha Atomic Research Centre, Bombay
42	***Form of distribution :***	Hard copy
50	***Language of text :***	English
51	***Language of summary :***	English
52	***No. of references :***	19 refs.
53	***Gives data on :***	
60	***Abstract :*** Fourier Spectra of 54 earthquake accelerograms recorded on rock sites in the U.S.A. have been analysed. These could be used in generation of synthetic accelerograms for seismic design.	
70	***Keywords/Descriptors :*** NUCLEAR POWER PLANTS; PLANNING; EARTHQUAKES; FOURIER ANALYSIS; USA; MATHEMATICAL MODELS; SEISMOLOGY; GROUND MOTION; SPECTRA; FOURIER TRANSFORMATION ; ALGORITHMS; ACCELERATION; DIAGRAMS	
71	***Class No. :*** INIS Subject Category : B31.40	
99	***Supplementary elements :***	

STUDIES ON FOURIER AMPLITUDE SPECTRA OF ACCELEROGRAMS RECORDED ON ROCK SITES

1. INTRODUCTION

Earthquake is an important consideration in the design of Nuclear Power Plants and other critical facilities like dams etc. The design basis earthquake ground motion is specified in terms of the following:-

(i) Peak ground acceleration
(ii) Response spectral shape
(iii) Time-history of ground acceleration

The motion is required to be specified in two orthogonal horizontal directions and in the vertical direction. The response spectral shapes for motion in the two horizontal directions are usually taken to be the same,

Several correlations exist for the determination of peak ground acceleration [see Campbell (1981) for a comprehensive review] in the horizontal direction. The ratio of the peak ground accelerations in various directions have been studied by several authors [Mohraz (1976), for example].

Site Independent Response Spectral Shapes for the ground motion have been recommended in some codes and guides [IAEA (1979), USAEC (1973), for example]. However, the site independent response spectral shapes recommended in the documents just mentioned have been found to be unconservative. Subsequently, response spectral shapes dependent on the site geology have been developed by several authors [Sced (1976), Mohraz (1976), Ghosh et.al (1986), (1987)].

The time-history of ground acceleration is required for time-history analysis of structures on ground and for generation of response spectra at various floor levels. Independent of the method of generation, this time-history generated responses spectrum (THRS) is required to be compatible with a specified design response spectrum (SDRS) [IAEA(1979)].

It has been felt that the use of the single spectrum-

compatible-accelerogram (SCA) may lead to unconservative floor response spectra [Singh (1975)].

This may happen since the SCA may not be rich in all the frequencies within the range of interest i.e. the energy content in each frequency-band may not be adequate. One way to circumvent this problem is to use multiple, typically about three to five, time-histories for generation of floor response spectra.

Alternatively, it has been suggested, one may use a single time-history if it is compatible with a SDRS as well as a specified power spectral density function (PSDF). [IEEE(1975), ASME (1986)].

There have been some suggestions in the literature about the target PSDF. One of the oldest forms is due to Kanai-Tajimi (1960) which gives the PSDF as

$$\text{PSDF} = S_o \frac{1 + 4\,\xi_g^2 \left(\frac{\omega}{\omega_g}\right)^2}{\left[1 - \left(\frac{\omega}{\omega_g}\right)^2\right]^2 + 4\,\xi_g^2 \left(\frac{\omega}{\omega_g}\right)^2} \qquad \ldots(1)$$

where,

S_o = 1100 in^2/sec^3 (this value corresponds to a peak acceleration of 1g), ω_g = 10.66 rad/sec and ξ_g = 0.9793.

However, the drawback of equation (1) stems from the fact that the PSD at zero frequency is non-zero, rather it has a high value. Thus, the same holds true for the Fourier Amplitude Spectrum (FAS) value as well. This will be untenable since this would imply a rather high ground acceleration as time tends to infinity. Further fixed values of ω_g and ξ_g leaves one with no choice to vary the PSDF depending upon the site conditions.

Clough and Penizen proposed the following model for the PSDF of the ground acceleration.

$$S_a(f) = S_o \left[\frac{1 + \left(2\,\xi_g \frac{f}{f_g}\right)^2}{\left[1 - \left(\frac{f}{f_g}\right)^2\right]^2 + \left(2\,\xi_g \frac{f}{f_g}\right)^2}\right] \left[\frac{\left(\frac{f}{f_k}\right)^4}{\left(1 - \frac{f}{f_k}\right)^2 + \left(2\,\xi_k \frac{f}{f_k}\right)^2}\right] \qquad \ldots(2)$$

...3..

The expression in the first bracket represents the low-pass Kanai-Tajimi filter, whereas the expression in the second bracket represents the high-pass Clough Penizen filter. The various parameters appearing in the equation (2) are determined empirically by matching the results from earthquake records, after they are normalised to unit spectral intensity. Use of spectral intensity (SI) as a normalising factor does not appear attractive as SI cannot be related well with other earthquake parameters in common use.

Unruh and Kana (1981) have proposed an iterative procedure for generation of response spectrum compatible PSDF. The work is based on the theory of random vibration. The PSDF can be generated to a specified level of confidence. However, the basic statistical distribution is not mentioned.

Shinozuka et al (1984) have also proposed an iterative procedure for generation of response spectrum compatible PSDF. However, the work is primarily based on Kanai-Tajimi's model.

The present work aims to develop target Fourier Amplitude Spectra (FAS) that could be used in design from the strong motion earthquake data. In view of the variations in spectral characteristics, as mentioned before, the records are grouped according to the geological condition (rock/soil) at site. Further, records of horizontal and vertical ground motion are treated separately. In this study FAS has been preferred to PSDF since PSDF depends on duration, which is often regarded as different from the length of the record, thus introducing some amount of subjectivity.

This report presents the results for FAS of earthquake accelerograms recorded on rock sites.

2. DATA SET

54 strong motion accelerograms (36 horizontal and 18 vertical components - from 7 earthquakes) recorded on rock sites in the

United States were considered for this study. The data were obtained as corrected accelerograms from the World Data Centre, Colorado. The geological conditions at the recording sites were obtained from various published sources. The salient features of the data are presented in Table - 1. Sr.Nos.9 - 14 correspond to the aftershocks of the San Fernando Earthquake of February 9, 1971.

The magnitude of the events considered were between 5 and 7 and the source distance varied, in general, between 20 - 60 kms. This is also the range of parameters considered (in general) in fixing the design basis earthquake for a site.

The accelerograms were first normalised with respect to the corresponding peak ground acceleration. The horizontal and the vertical components were treated separately.

3. THEORY

The Fourier Transform X(f) of Signal x(t) of duration T is given as [Champeney, 1969].

$$X(f) = \int_0^T x(t)\, e^{-j2\pi ft}\, dt \quad , \quad j = \sqrt{-1} \qquad \ldots(3a)$$

and the inverse is given by

$$x(t) = \int_0^F x(f)\, e^{j2\pi ft}\, dt \qquad \ldots(3b)$$

when x(t) is discretised at N points at an interval of Δt and there are as many points considered in the frequency domain.

$$\Delta f = \frac{1}{N\Delta t}$$

Equation (3a) is written in the discrete form as

$$x(k\Delta f) = \Delta t \sum_{n=0}^{N-1} x(n\Delta t)\, e^{-j2\pi (k\Delta f).n\Delta t}$$

$$= \Delta t \sum_{n=0}^{N-1} x(n\Delta t)\, e^{-\frac{j2\pi kn}{N}} \qquad \ldots(4)$$

...5..

$k = 0,1,2, \ldots N-1$

$= C_k - j Q_k$ (say)

$$C_k = \Delta t \sum_{n=0}^{N-1} x(n\Delta t) \cos(an) \qquad \ldots(5)$$

$$Q_k = \Delta t \sum_{n=0}^{N-1} x(n\Delta t) \sin(an) \qquad \ldots(6)$$

$$a = \frac{2\pi k}{N}$$

Then Fourier Amplitude Spectrum at frequency $f_k = k\Delta f$ is obtained as

$$FAS(f) = (C_k^2 + Q_k^2)^{1/2} \qquad \ldots(7)$$

The PSDF at the frequency f is defined as

$$PSDF(f) = \frac{[FAS(f)]^2}{T} \qquad \ldots(8)$$

However, the discrete FAS will be accurate only upto

f = fmax/2. [Champeney (1969)].

The following activities were planned.

(i) Evaluation of the FAS of each individual accelerogram at Δf dictated by the length of the particular record and interpolating the values at selected frequencies which would be common for all.

(ii) Truncating all the records beyond a fixed time duration say, the least value observed in the data set (To).

(iii) Expanding all the records to a fixed duration - say, the maximum value observed in the data set (Tm) by padding a number of zeros to a record.

The first method, however, can significantly alter the

...6..

spectral shape depending upon the difference in frequency interval in the two sets of computations. Several spectral peaks are also likely to be missed. A typical illustration is given in Fig.1.

The second method implies multiplication of the signal by a box-car function [say, $y(t)$]. A two sided box-car function and its transform are shown in Figs.2 and 3 [Kelly and Richman (1969)]. However, the same concepts can be applied for a one-sided function and its transform as well. It can be shown that the Fourier amplitude spectra for both the cases are identical.

$$y(t) = 1 \qquad 0 \leq T \leq To$$
$$= 0 \qquad T > To \qquad \ldots(9)$$

Thus, the Fourier Transform of the resulting function will be, by Parseval's theorem

$$F\left[x(t).y(t)\right] = F\left[x(t)\right] * F\left[y(t)\right] = X(f) * Y(f)$$

$F\left[X(t)\right]$ denotes the Fourier Transform of $x(t)$ and $*$ denotes convolution.

Hence,

$$F\left[x(t).y(t)\right] = \int_0^f x(g).Y(f-g)\,dg \qquad \ldots(10)$$

The distortion due to truncation of a signal is thus evident from equation (10). A typical illustration is shown in Fig.4.

However, the third method does not introduce any significant error. This can be shown analytically. For convenience, let us consider that for the original signal $x(t)$ of duration T $N = 2$. Then there are two samples of the time-history, x_0 and x_1. Hence, the discrete Fourier Transforms are:

$$X(0) = \Delta t\left[x_0 + x_1\right] \qquad \ldots(11)$$

$$X(1) = X\left(\frac{1}{2\Delta t}\right) = \Delta t\left[x_0 + x_1 e^{-j\pi}\right] \qquad \ldots(12)$$

Now let us pad the time-history with $x_2 = 0$ and $x_3 = 0$ so that $N = 4$.

In this case,

$$\Delta f = \frac{1}{4\Delta t} \qquad \ldots(13)$$

$$X(0) = \Delta t\left[x_0 + x_1 + x_2 + x_3\right] = \Delta t\,(x_0 + x_1)$$

$$X\left(\frac{1}{4\Delta t}\right) = \Delta t\left[\sum_{n=0}^{3} x_n\, e^{-\frac{j\pi n}{2}}\right] \qquad \ldots(14)$$

$$X\left(\frac{2}{4\Delta t}\right) = X\left(\frac{1}{2\Delta t}\right) = \Delta t\left[\sum_{n=0}^{3} x_n\, e^{-j\pi n}\right]$$

$$= \Delta t\left[x_0 + x_1 e^{-j\pi} + x_2 e^{-j2\pi} + x_3 e^{-j3\pi}\right] = \Delta t\left[x_0 + x_1^{-j}\right] \qquad \ldots(15)$$

Equations (11) and (13) are identical i.e. X(0) is unchanged due to padding with zeros. Similarly equations (12) and (15) are identical hence X(1) is also unchanged.

In this case the frequency points for N = 2 were considered for N = 4 as well. In a simple problem it can be shown that even if this condition is not satisfied the Fourier Spectrum is not significantly distorted. However, since analytical solution cannot be extended for large values of N, this was studied numerically with several actual records and the observation was found to be valid. A typical illustration is shown in Fig.5.

For the maximum record length N was 3270 - hence all the accelerograms were extended to 3270 points (Δt = 0.02 sec) by padding with the requisite number of zeros.

For faster computation with FFT algorithm (of the Cooley-Tukey type) one would have needed N as a power of 2, necessitating truncation of records (for N = 2048) or padding by many more zeros (for N = 4096) and resulting in higher distortion of the spectra. Hence, it was necessary to compute the discrete Fourier Transform by some other algorithm. For economy of computational time, a recursive algorithm was used. This is given in the Appendix.

The FAS, normalised to corresponding peak around acceleration, were computed for all the records. At each frequency the

mean value (M) the standard deviation (σ) and the maximum value were computed. Mean, Mean plus Sigma and Envelope Spectra of horizontal and vertical motions were evaluated separately.

4. NUMERICAL RESULTS AND DISCUSSION

Some representative normalised FAS are shown in Figs. 6 - 13. In general, the spectral amplitudes are significant in the frequency range 0.5 - 10 Hz and the decay beyond 10 Hz is rapid. For the same magnitude of earthquake, the peak spectral amplitude occurs at a lower frequency as the source distances increases. For a fairly large magnitude, significant peaks are more closely spaced as the distance increases (Ref. Figs. 6 - 9).

For the same distance, the spectral peak shifts to a higher frequency with reduction in magnitude (Ref. Figs.6, 10 and 11). For higher magnitude and greater source distance the spectral peak shifts to a lower frequency (Ref. Figs. 12 and 13).

The examples presented are for the horizontal component of ground motion. These general trends are observed for the corresponding vertical components as well. However, for brevity these results are not presented.

The mean and the standard deviation of the ensemble of the normalised Fourier Amplitude Spectra were evaluated at each frequency to obtain the mean and mean plus sigma spectra. The envelope spectra were obtained from the maximum spectral amplitude of the ensemble. These results are presented in Figs.14 through 17.

It is observed that, for a comparable confidence level, the spectrum for vertical motion has its peak at a frequency higher than that for the spectrum of horizontal motion. However, the spectrum of vertical motion is richer in the low frequency range.

The zero-frequency-component of each of the horizontal and the vertical spectra are zero. Comparison of the PSDs computed from the mean FAS for 1g peak acceleration and 10 seconds duration with the PSDF proposed by Kanai-Tajimi are shown in Figs.18 and 19. Target PSDs having confidence level of 84% and compatible with 5% damping, mean plus sigma spectra of horizontal and vertical ground

motion on rock sites (Ghosh et al, 1986) were also computed following the procedure suggested by Unruh and Kana. These are also plotted in Figs. 18 and 19.

These PSDs and the ones obtained in the present study show similar trends i.e. they tend to zero in the very low and very high frequency range. They also show a relatively higher bandwidth compared to the Kanai-Tajimi form of the PSD. The difference in the amplitudes of FAS or PSD derived in this study and those from Kana-Unruh's procedure may be attributed to the phase distribution implicit in the latter. It may be noted that the phase distribution considered in this study are those of the actual records.

Using target Fourier Amplitude Spectrum one can obtain an artificial accelerogram by inverting the Fourier transform. The phase distribution may be chosen so that the THRS is compatible with SDRS and the accelerogram can be made to satisfy other constraints e.g. time to peak acceleration, duration etc.

Choice of FAS as a working parameter is more attractive than PSD since duration of the earthquake is not required to be explicitly specified.

ACKNOWLEDGEMENTS

The authors thank Shri N.N. Kulkarni, Consultant, NPC and Prof. A.R. Chandrasekaran, DEQ, University of Roorkee for many stimulating discussions. They also thank Dr. Lollah. G.K. Murthy, Head, RASD, BARC, for his encouragement.

REFERENCES

1. ASME (1986) - Boiler and Pressure Vessel Code, Sec III, American Society of Mechanical Engineers.

2. Campbell, K.W. (1981) - Near Source Attenuation of Peak Horizontal Acceleration, Bulletin of the Seismological Society of America, 71(6), 2039-2070.

3. Champeney, D.C. (1973) - Fourier Transforms and Their Physical Applications - Academic Press, N.Y.

4. Chough, R.W. and J. Penizen (1975), Dynamics of Structures, McGraw Hill, New York.

5. Ghosh, A.K., R.D. Sharma and N. Muralidharan (1986), Spectral Shapes for Accelerograms Recorded at Rock Sites, Report BARC - 1314, Bhabha Atomic Research Centre, Government of India, Bombay, India.

6. Ghosh, A.K. and R.D. Sharma (1987), Spectral Shapes for Accelerograms Recorded at Soil Sites, Report BARC - 1365, Bhabha Atomic Research Centre, Government of India, Bombay, India.

7. IAEA (1979) - Earthquakes and Associated Topics in Relation to Nuclear Power Plant Siting, Safety Guide 50 - SG - S1, IAEA, Vienna.

8. IEEE (1975) - IEEE Recommended Practices for Seismic Qualification of Class IE Equipment for Nuclear Power Generating Stations, ANSI/IEEE Std. 344 - 1975, IEEE.

9. Joyner, W.B. and D.M. Boore (1981) - Peak Horizontal Acceleration and Velocity from Strong Motion Records Including Records from the 1979 Imperial Valley, California Earthquakes, Bulletin of the Seismological Society of America, 71(6), 2011-2038.

10. Kanai, K. (1957) - Semi-empirical Relation for the Seismic Characteristics of the Ground, Bulletin of the Earthquake Research Institute, Tokyo University, 35, 308 - 325.

11. Kelly, R.D. and G. Richman (1969) - Principles and Techniques of Shock Data Analysis, SVM - 5, The Shock and Vibration

Information Centre, U.S. Dept. of Defence.

12. Mohraz, B. (1976) - A Study of Earthquake Response Spectra for Different Geological Conditions, Bulletin of the Seismological Society of America, 63, 915 - 935.

13. Seed, H.B., C. Ugas and J. Lysmer (1976) - Site Dependent Spectra for Earthquake Resistant Design, Bulletin of the Seismological Society of America, 66, 221 - 243.

14. Seed, H.B., R. Murarka, J. Lysmer and I.M. Idris (1976) - Relationship of Maximum Acceleration, Maximum Velocity, Distance from Source and Local Site Conditions for Moderately Strong Earthquakes, Bulletin of the Seismological Society of America, 66, 1323 - 1342.

15. Singh, M.P. (1975) - Generation of Seismic Floor Spectra, Jl. of Engineering Mechanics Division, Proc. ASCE, 101EM5, 593-607.

16. Shimozuka, M., T. Mochio and E.F. Samaras (1984) Power Spectral Density Functions Compatible with NRC RG 1.60 Response Spectra, NURG/CR - 3509.

17. Tajimi, H. (1960) - A Statistical Method of Determining the Maximum Response of a Building Structure During an Earthquake - Proc. 2nd World Conference on Earthquake Engineering, Tokyo and Kyoto, Japan, 781 - 797.

18. Unruh, J.P. and D.D. Kana (1981) - An Iterative Procedure For The Generation of Consistent Power/Response Spectrum - Nuclear Engineering and Design, 66, 427 - 435.

19. USAEC (1973) - Design Response Spectra for Seismic Design of Nuclear Power Plants, Regulatory Guide 1.60, U.S. Atomic Energy Commission, Directorate of Regulatory Standards.

T A B L E - 1

DATA BASE FOR THE PRESENT STUDY

Sl. No.	Earthquake	Station Name & No.	Mag.	Source Dist(Km)	Component	Acc (g)	Source +
1.	Kern county 21/07/52	Taft, CAL 1095	7.6	56.0	N21E S69E Vert	.156 .179 .105	Seed et al (1976)
2.	SanFrancisco 22/03/57	Golden Gate 1077	5.25	11.0	N10E S80E Vert	.083 .105 .038	Seed et al (1976)
3.	Helena Mnt 31/10/35	Federal Bldg Helana, 323	6.0	8.0	S00W S90W Vert	.146 .145 .089	Seed et al (1976)
4.	WheelerRidge 12/01/1954	Taft, CAL 1095	6.0	51.0	N21E S69E Vert	.064 .067 .036	Seed et al (1976)
5.	Parkfield 27/06/66	Temblor, CAL 1097	5.6	7.0	N65W S25W Vert	.269 .347 .132	Seed et al (1976)
6.	Parkfield 27/06/66	San Luis 1083	5.6	63.6	N36W S54W Vert	.018 .013 .006	Joyner & Boore (1981)
7.	Borrego Mtn 08/04/68	SCE Plant 280	6.5	122.0	N33E N57W Vert	.041 .046 .055	Seed et al (1976)
8.	San Fernando 09/02/71	Pacoima Dam 279	6.6	3.2	S16E S74W Vert	1.250 1.240 .709	Campbell (1981)
9.	San Fernando 09/02/71	Pacoima Dam 279	2.4	3.2	S16E S74W Vert	.021 .027 .008	Campbell (1981)
10.	San Fernando 09/02/71	Pacoima Dam 279	3.1	3.2	S16E S74W Vert	.052 .046 .021	Campbell (1981)
11.	San Fernando 09/02/71	Pacoima Dam 279	4.0	3.2	S16E S74W Vert	.115 .112 .041	Campbell (1981)

Sl. No.	Earthquake	Station Name & No.	Mag	Source Dist.(Km)	Component	ACC (g)	Source
12.	San Fernando 09/02/71	Pacoima Dam 279	3.0	3.2	S16E S74W Vert	.032 .048 .015	Campbell (1981)
13.	San Fernando 09/02/71	Pacoima Dam 279	2.5	3.2	S16E S74W Vert	.031 .024 .024	Campbell (1981)
14.	San Fernando 09/02/71	Pacoima Dam 279	2.4	3.2	S16E S74W Vert	.028 .019 .007	Campbell (1981)
15.	San Fernando 09/02/71	Castiac Old 110	6.6	22.8	N21E N69W Vert	.390 .320 .156	Campbell (1981)
16.	San Fernando 09/02/71	LA Water & Power, 137	6.6	24.1	N50W S40W Vert	.200 .140 .068	Campbell (1981)
17.	San Fernando 09/02/71	LA2011 Zonal 190	6.6	25.5	S62E S28W Vert	.080 .070 .050	Campbell (1981)
18.	San Fernando 09/02/71	Pmp Pt, Pearblossom 269	6.6	35.5	N00E N90W Vert	.150 .100 .048	Campbell (1981)

+Source for verifying Geological Conditions.

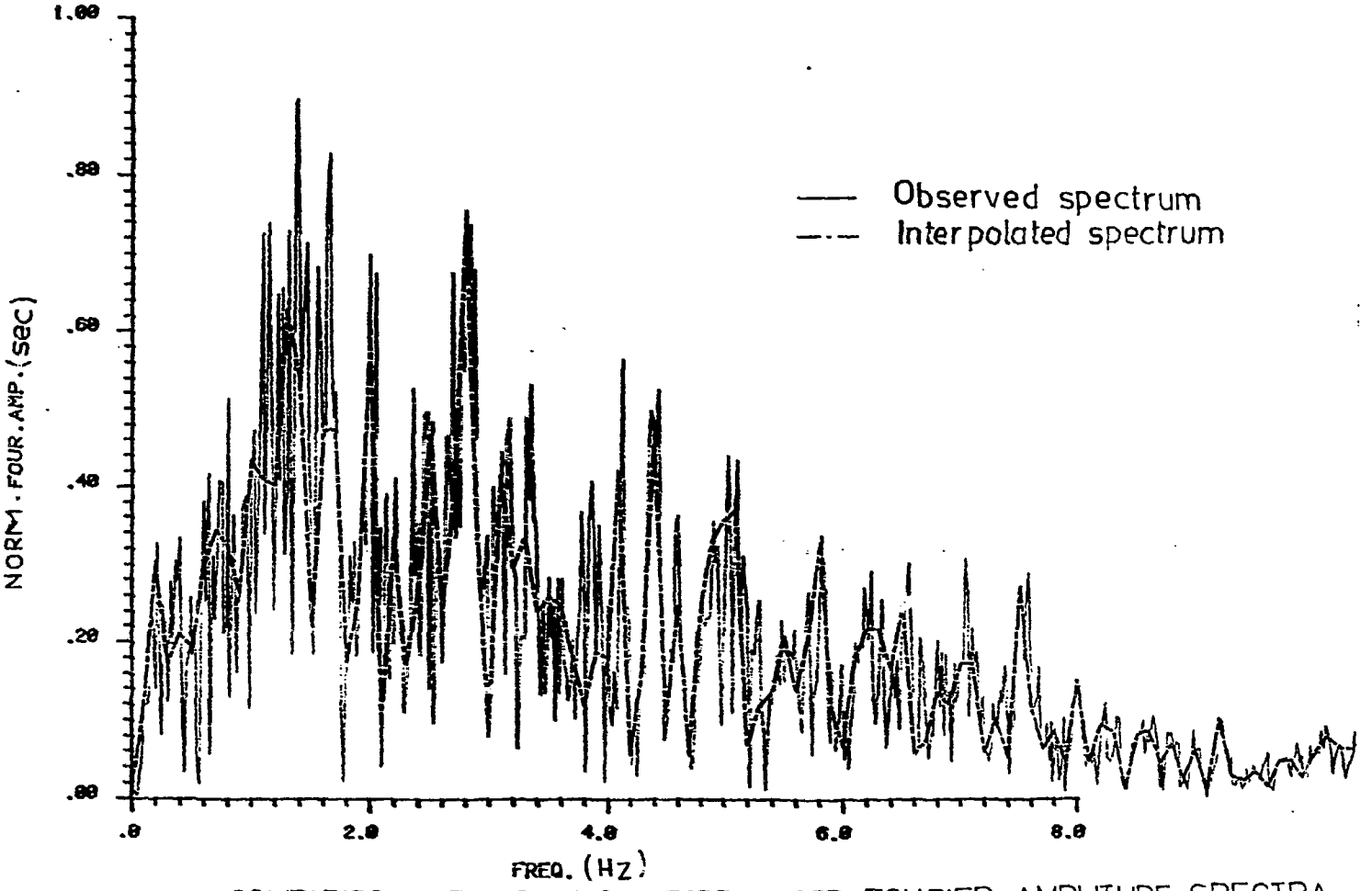

FIG.1: COMPARISON OF ACTUAL & INTERPOLATED FOURIER AMPLITUDE SPECTRA
(N21E Component of item 1 in Table-1)

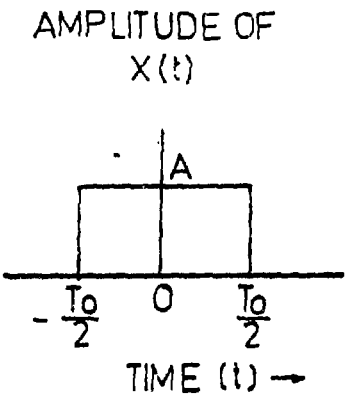

$$X(t) = \begin{cases} A & -\frac{T_0}{2} \leq t \leq \frac{T_0}{2} \\ 0 & \text{elsewhere} \end{cases}$$

Fig.2: A BOXCAR TIME FUNCTION

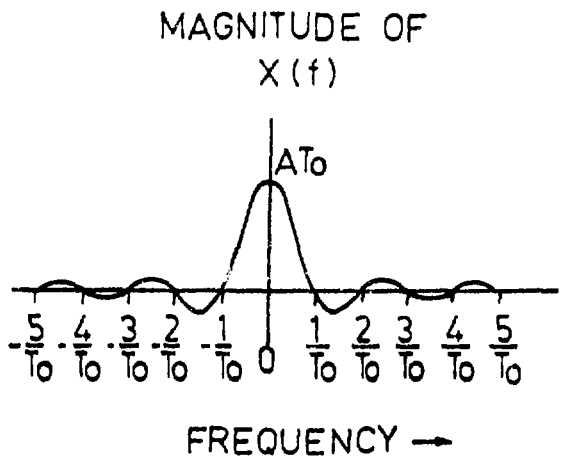

$$X(f) = (ATo)\left[\frac{\sin(\pi f To)}{\pi f To}\right]$$

Fig.3: A BOXCAR FREQUENCY FUNCTION

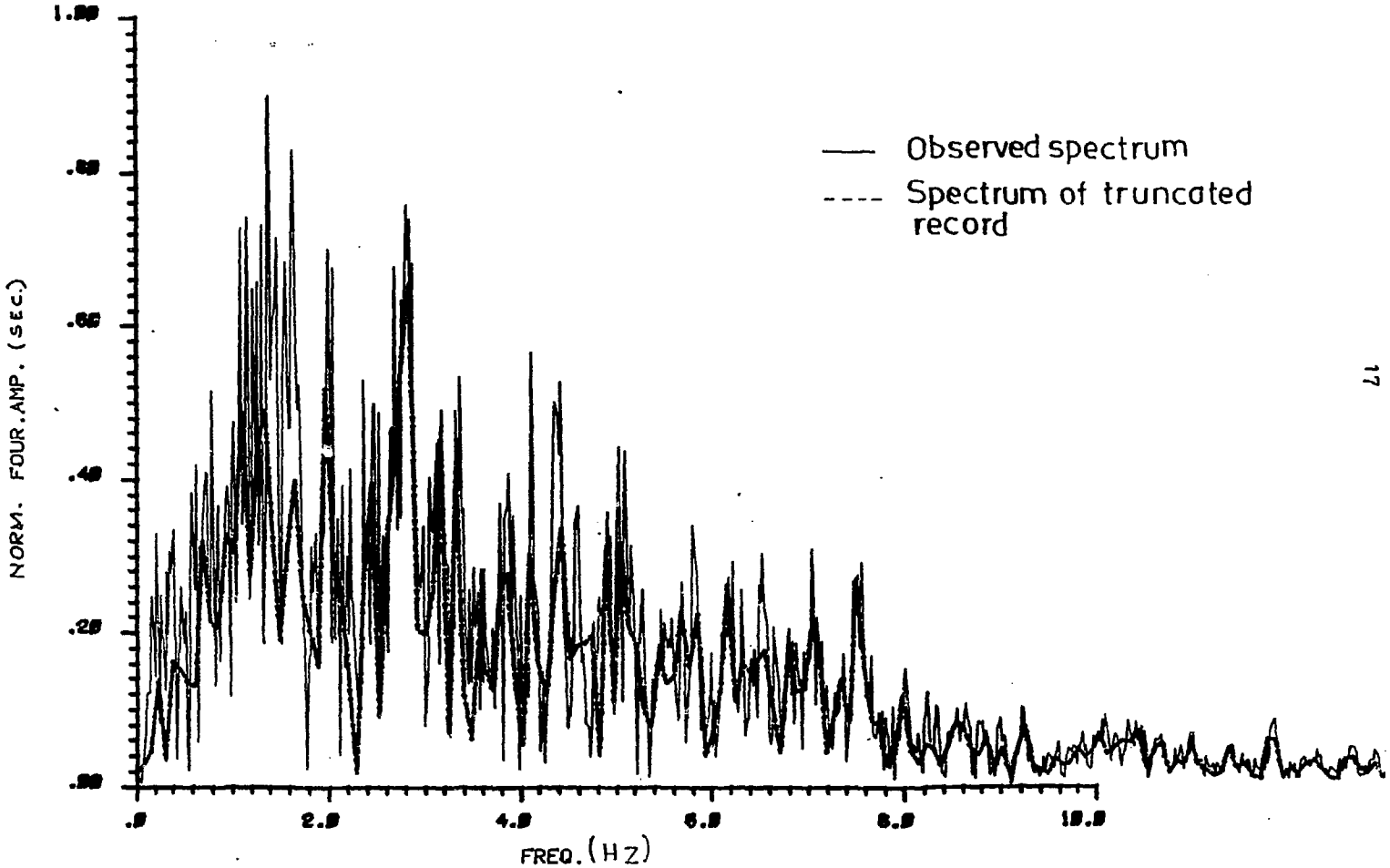

Fig. 4. COMPARISON OF FOURIER AMPLITUDE SPECTRA OF ACTUAL AND TRUNCATED ACCELEROGRAMS (N21E Compnent of item 1 in Table-1)

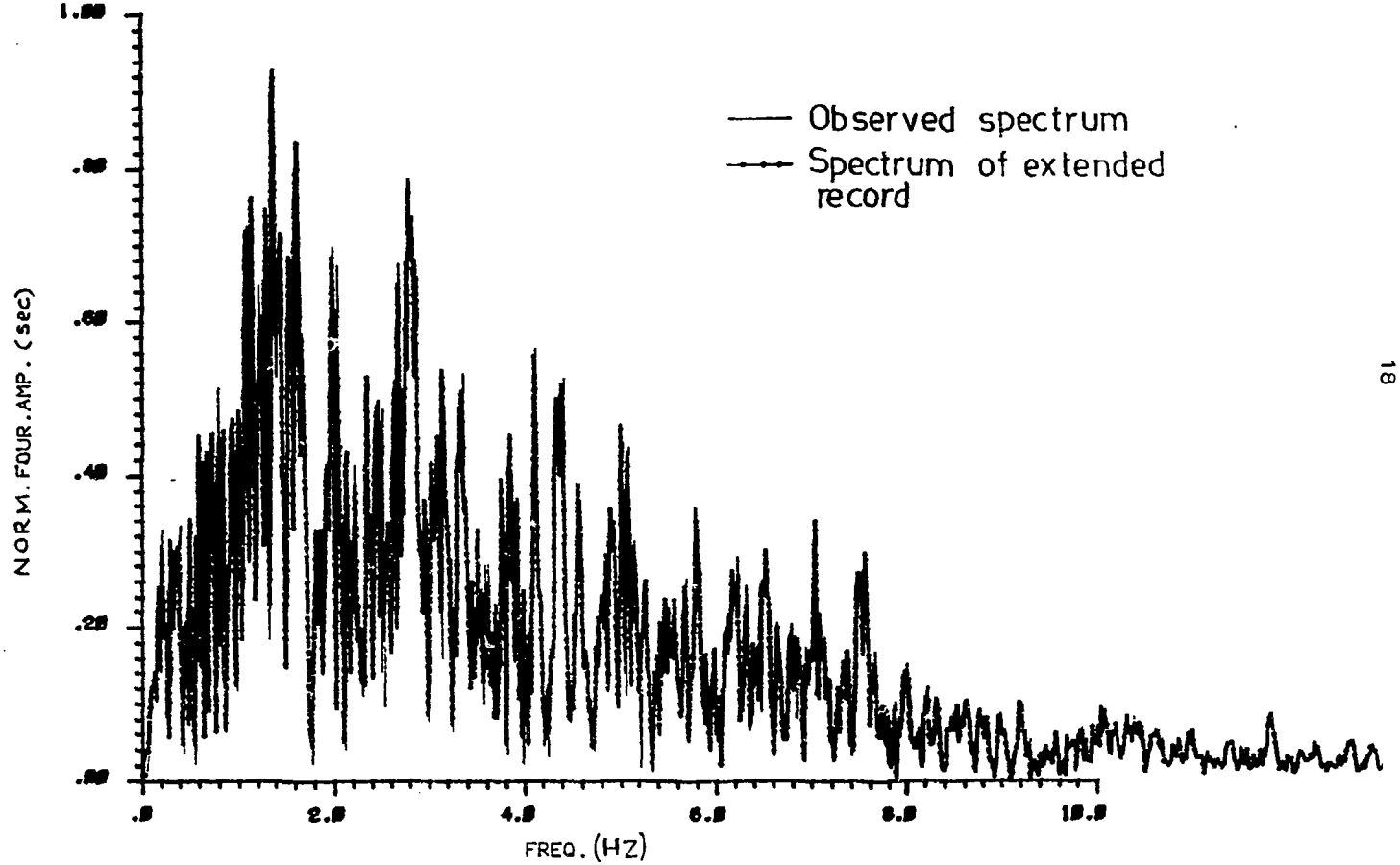

Fig.5 COMPARISON OF FOURIER AMPLITUDE SPECTRA OF ACTUAL & EXTENDED ACCELEROGRAMS (N21E Component of item 1 in Table-1

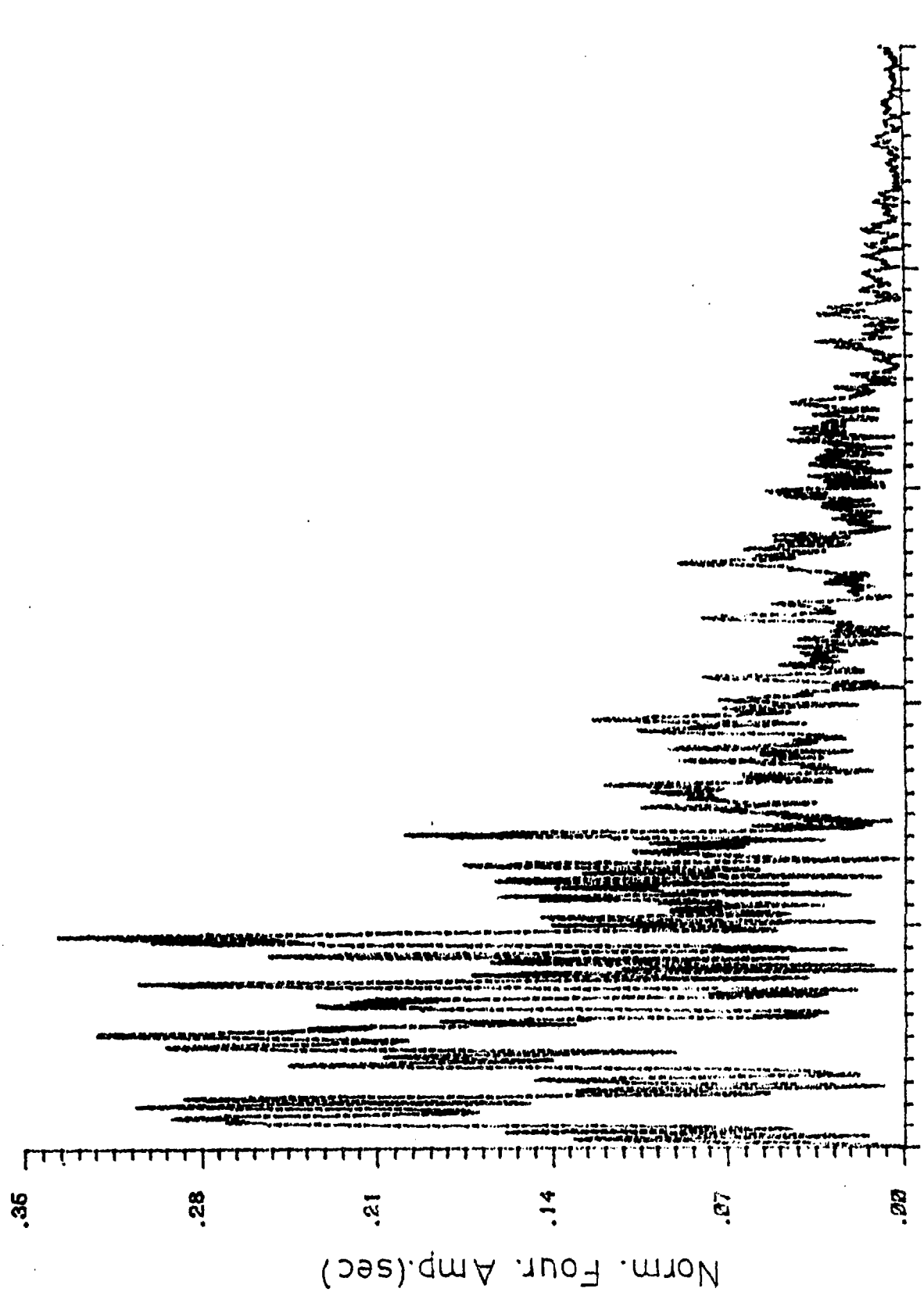

Fig. 6: NORMALISED FOURIER AMPLITUDE SPECTRUM OF ACCELEROGRAM (S16E Component of item 8 in Table-1)

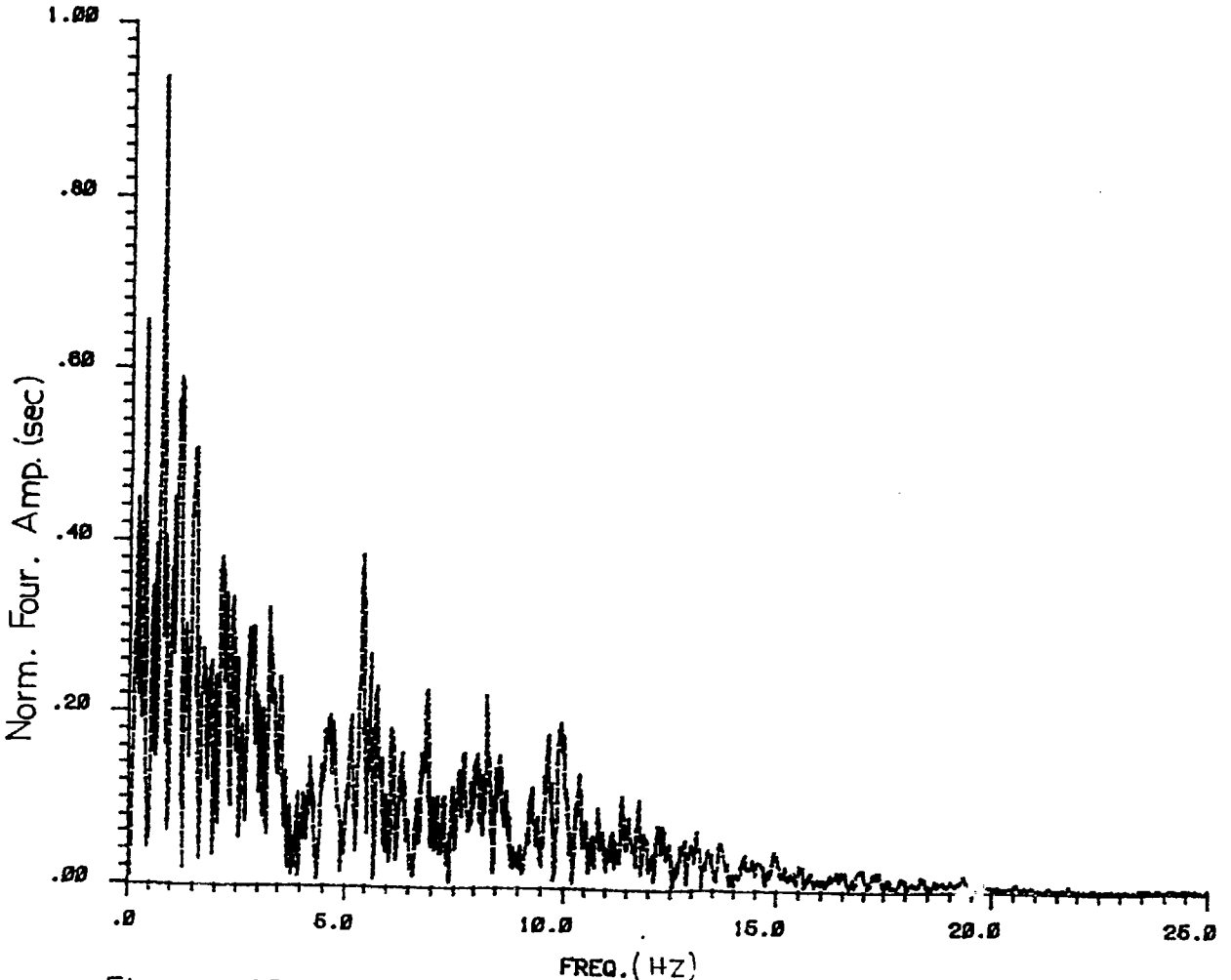

Fig.7 : NORMALISED FOURIER AMPLITUDE SPECTRUM OF ACCELEROGRAM (N50W Component of item 16 in Table_1

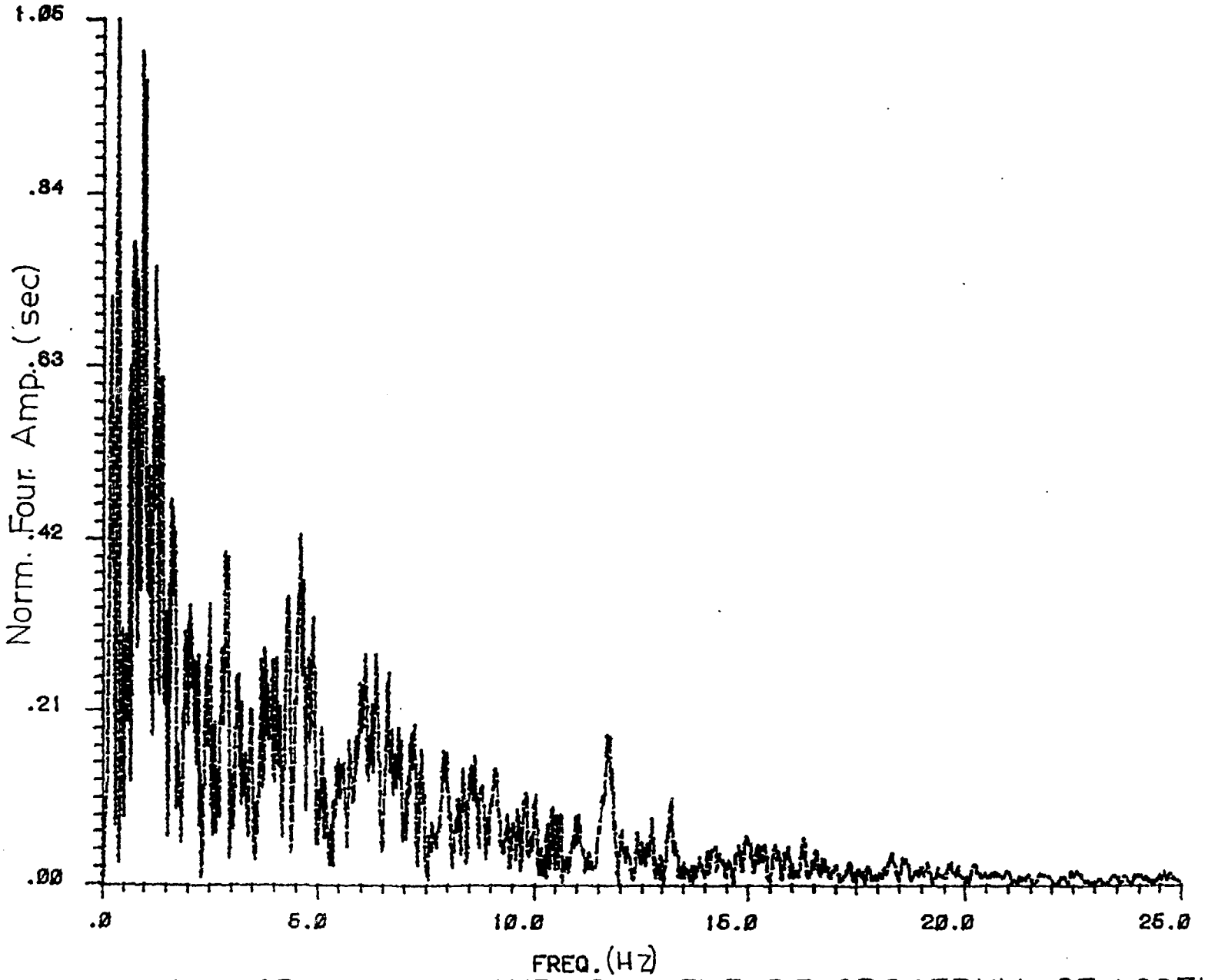

Fig. 8 : NORMALISED FOURIER AMPLITUDE SPECTRUM OF ACCELEROGRAM

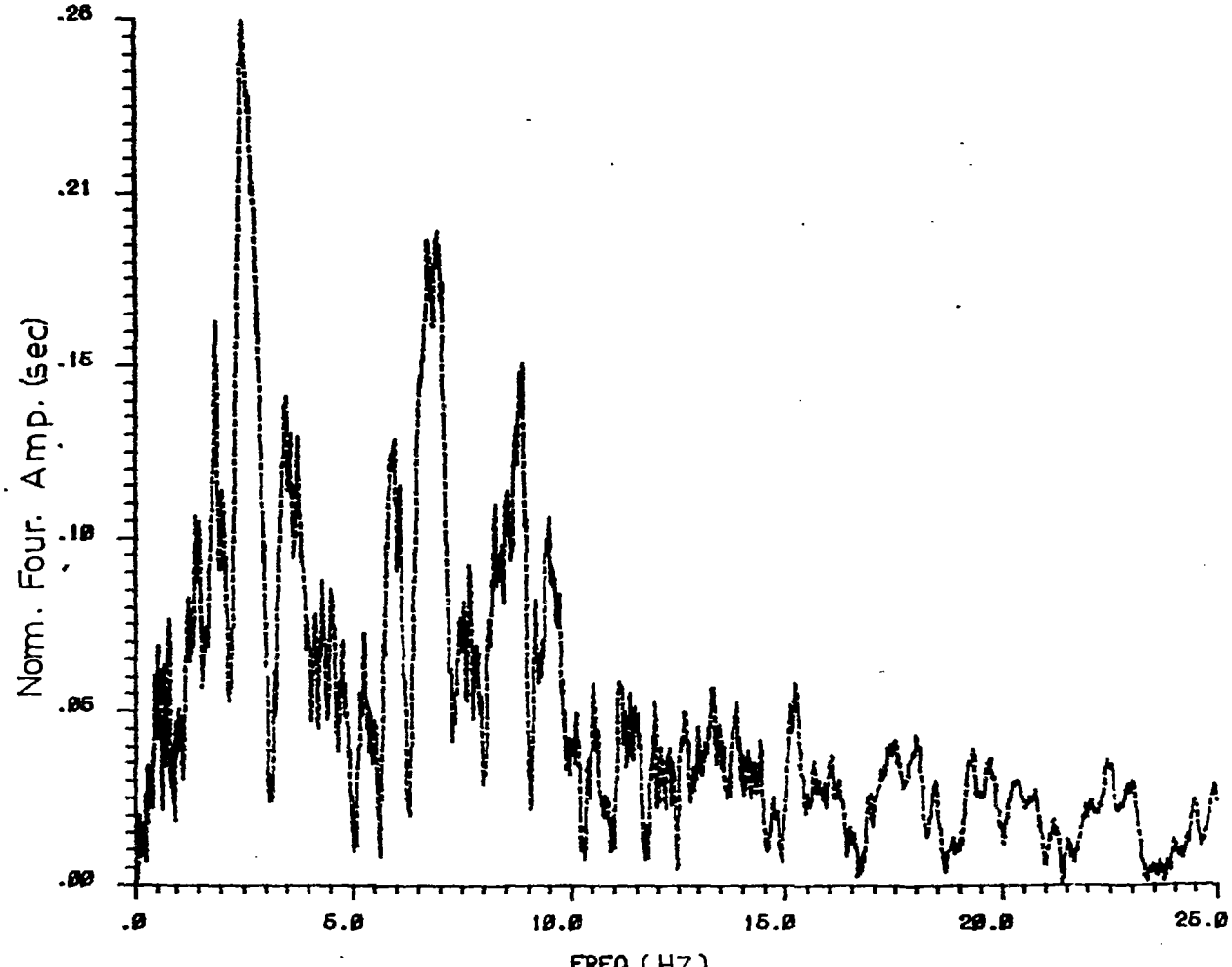

Fig.9: NORMALISED FOURIER AMPLITUDE SPECTRUM OF ACCELEROGRAM (S00W Component of item 3 in Table-1)

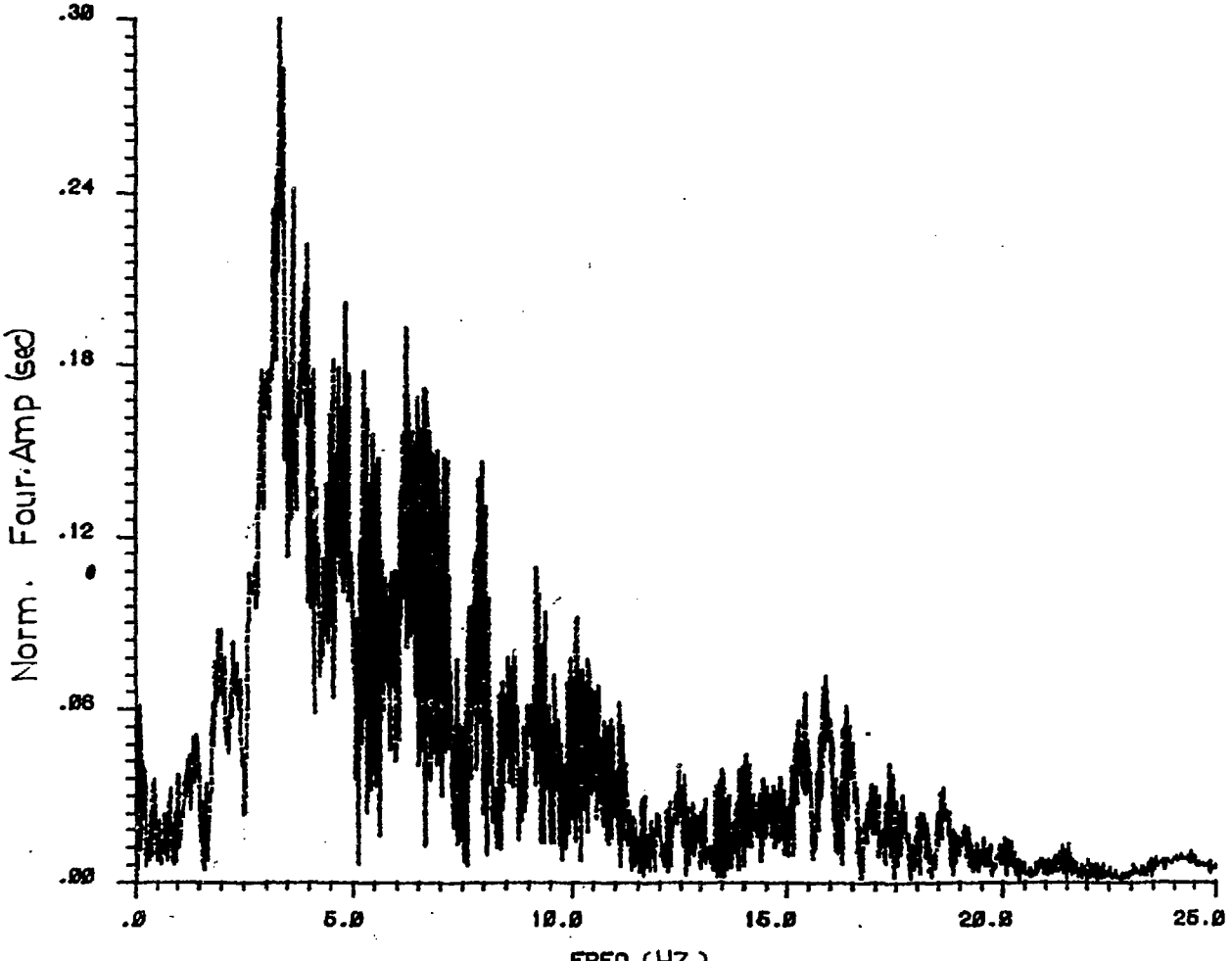

Fig.10: NORMALISED FOURIER AMPLITUDE SPECTRUM OF ACCELEROGRAM (S16E Comp. of item 11 in Table-1

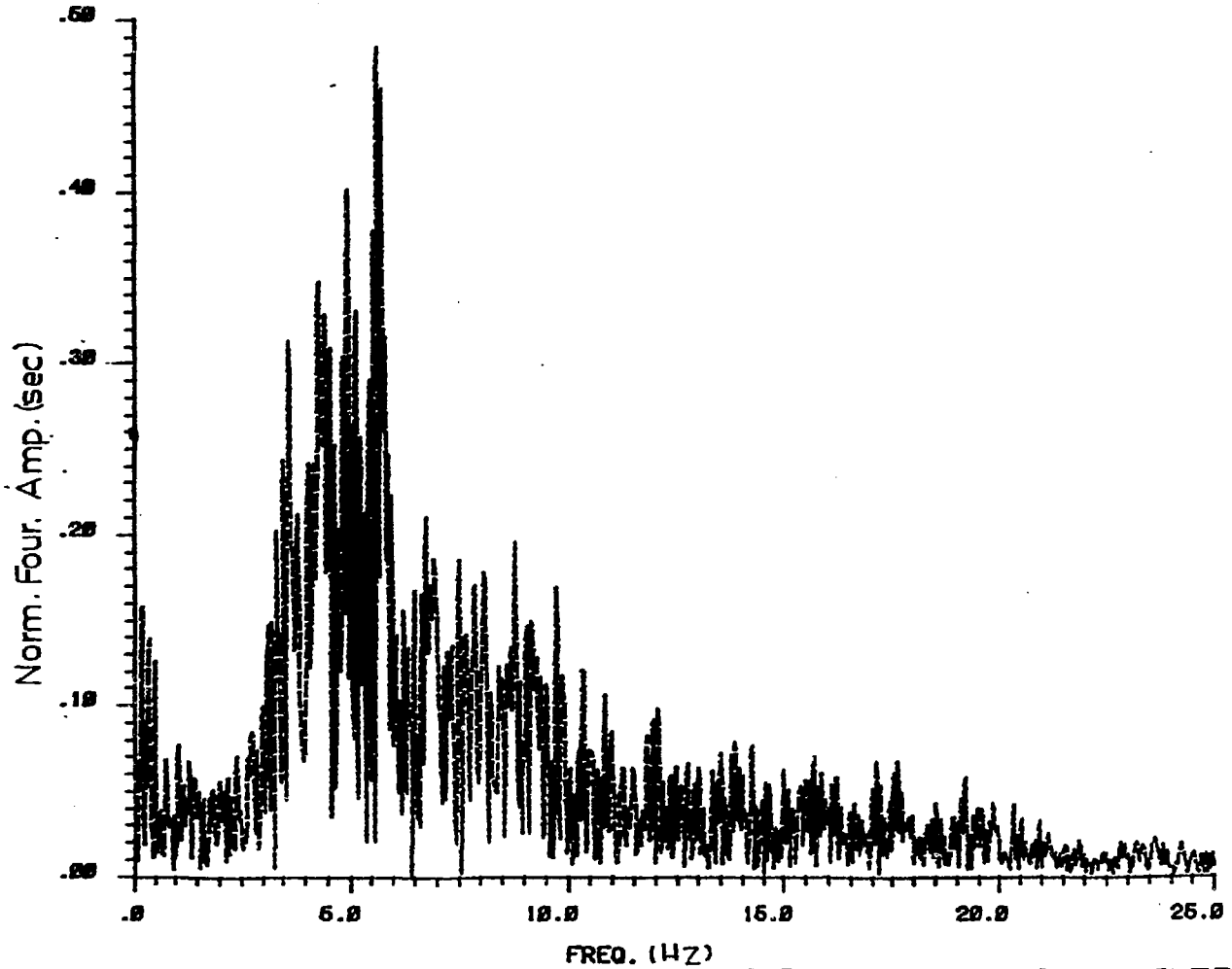

Fig.11: NORMALISED FOURIER AMPLITUDE SPECTRUM OF ACCELEROGRAM (S16E Component of item 13 in Table-1)

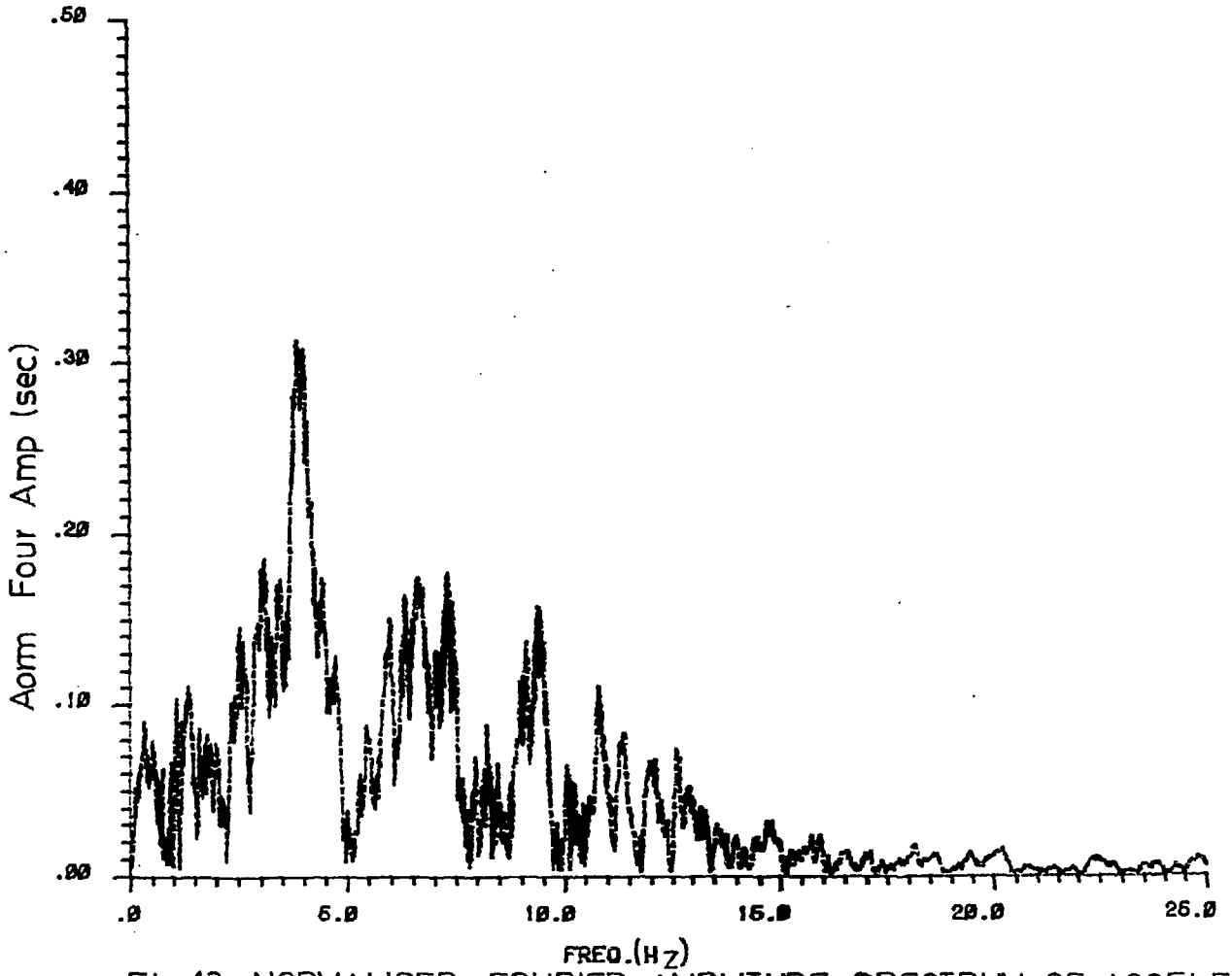

Fig.12 : NORMALISED FOURIER AMPLITUDE SPECTRUM OF ACCELEROGRAM (N10E Component of item 2 in Table_1)

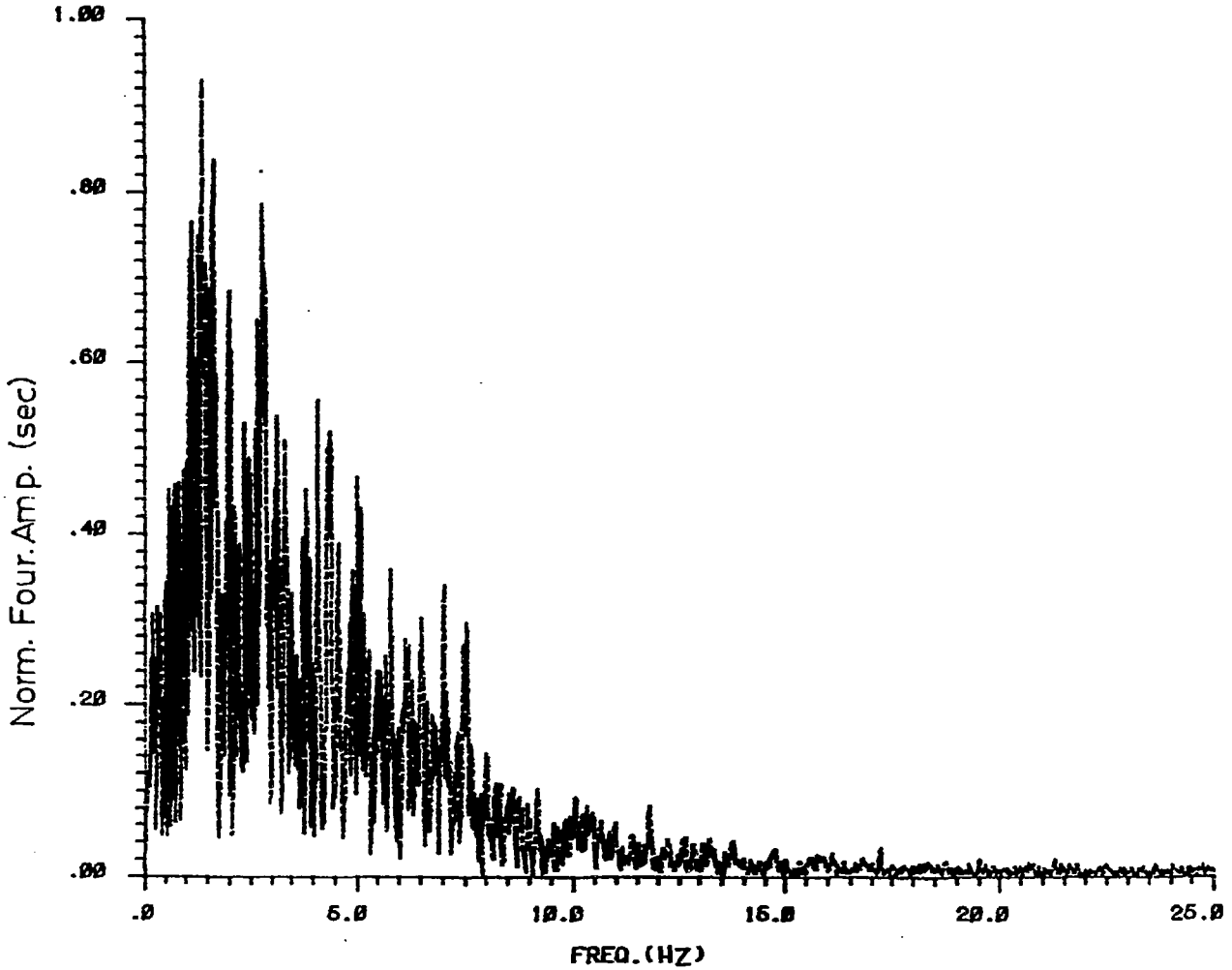

Fig.13: NORMALISED FOURIER AMPLITUDE SPECTRUM OF ACCELEROGRAM
(N21E Component of item 1 in Table-1)

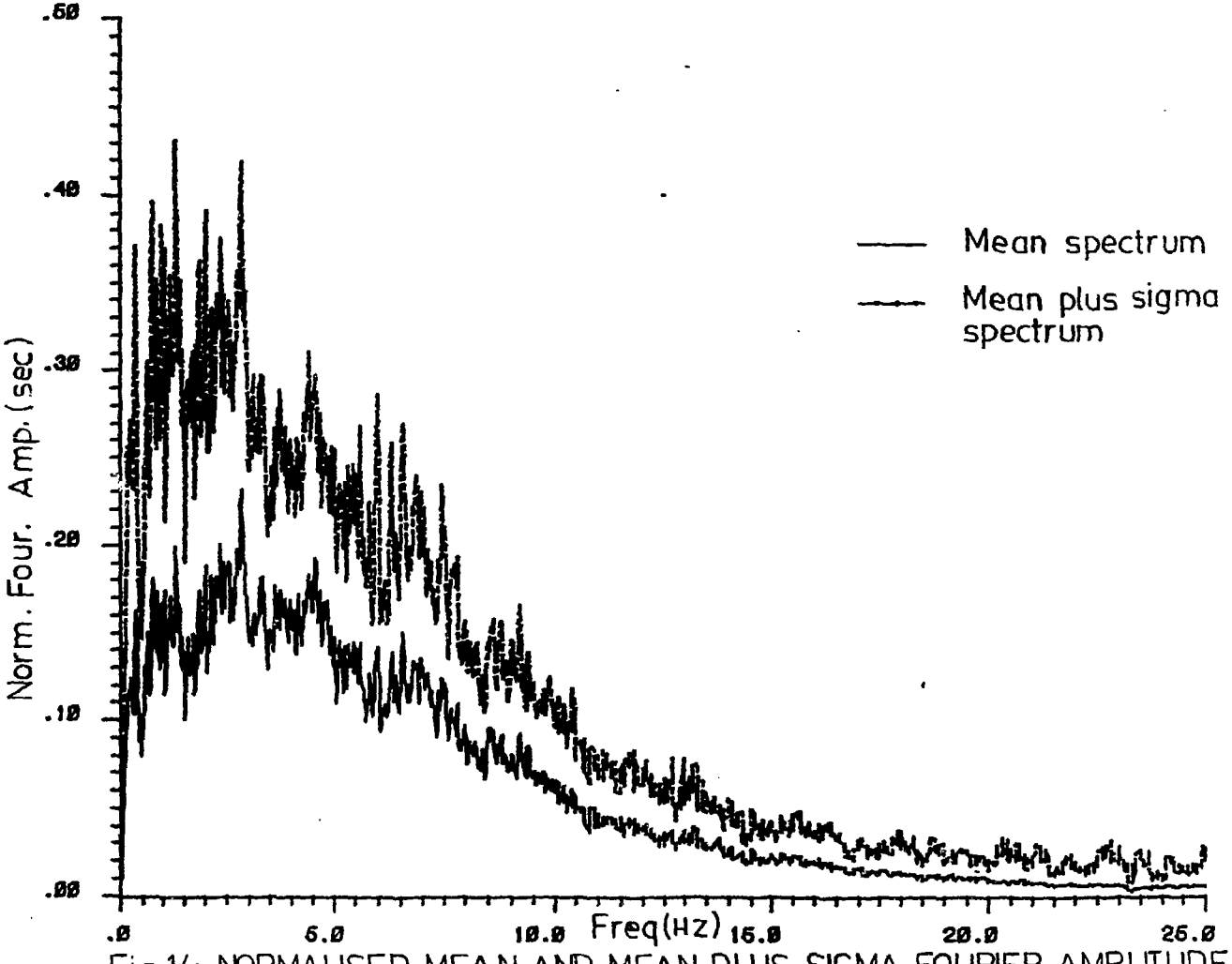

Fig.14: NORMALISED MEAN AND MEAN PLUS SIGMA FOURIER AMPLITUDE SPECTRA FOR HORIZONTAL COMPONENT OF GROUND MOTION (Rock sites)

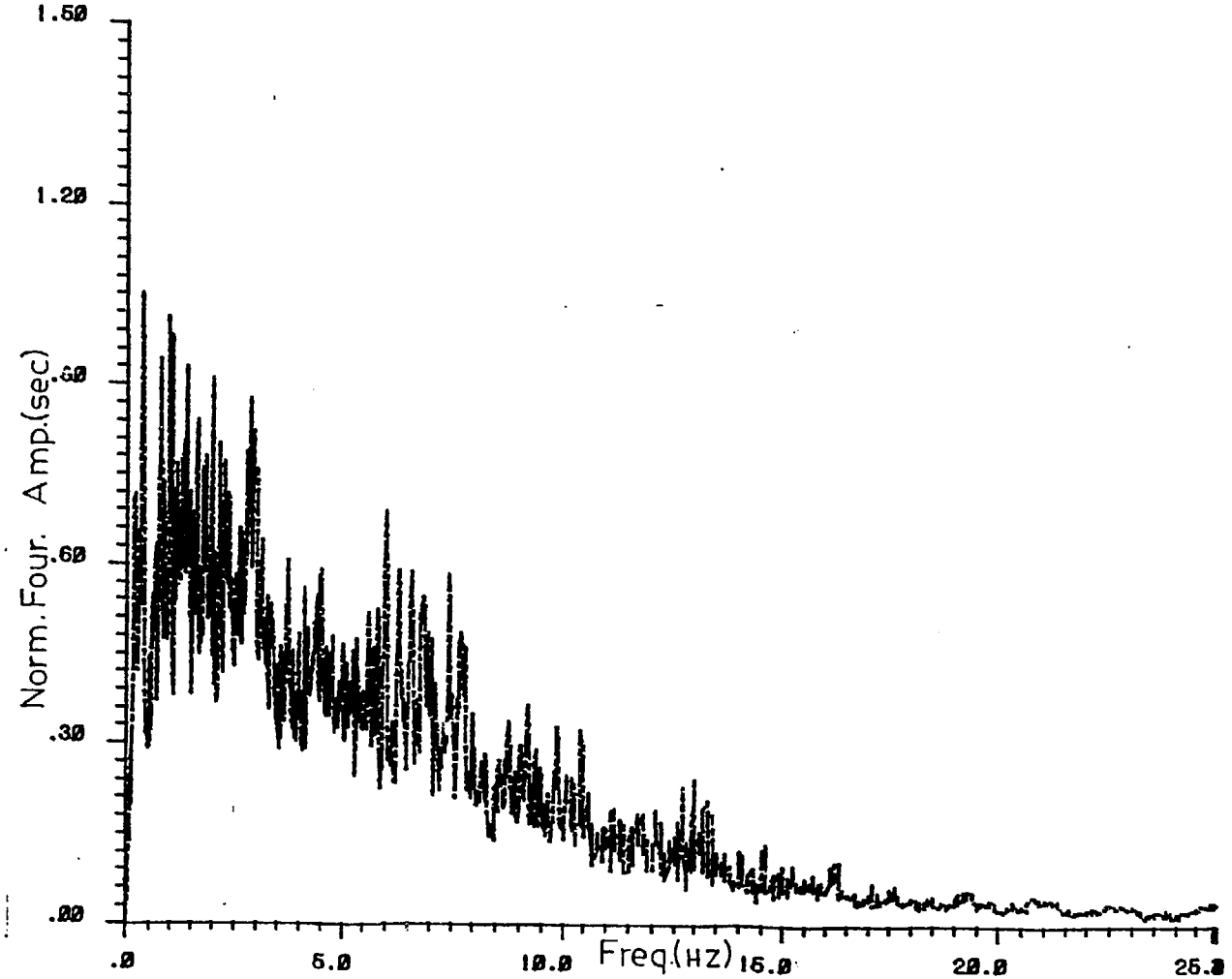

Fig.15: NORMALISED ENVELOPING FOURIER AMPLITUDE SPECTRUM FOR HORIZONTAL COMPONENT OF GROUND MOTION (Rock sites)

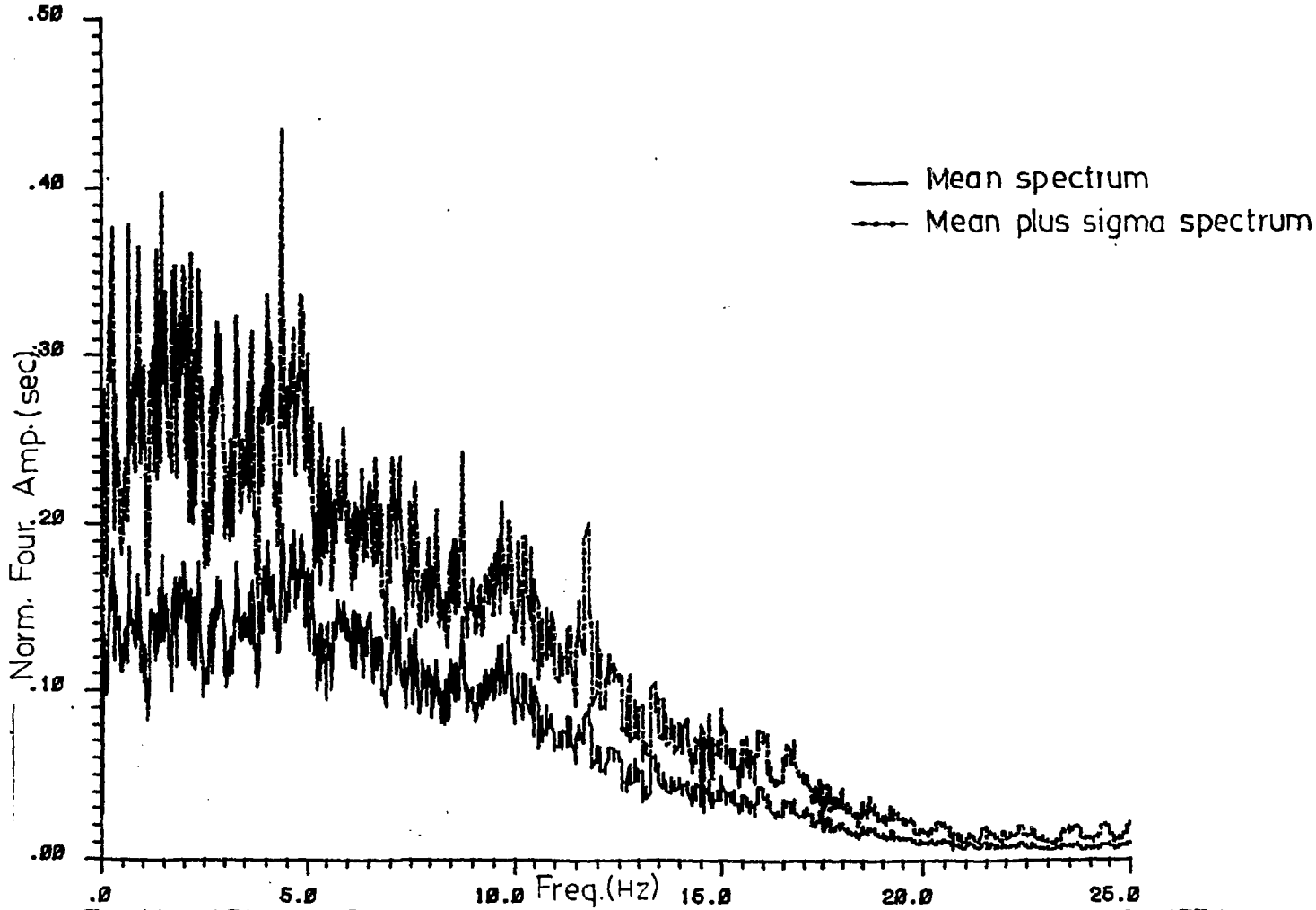

Fig.16 : NORMALISED MEAN AND MEAN PLUS SIGMA FOURIER AMPLITUDE SPECTRA FOR VERTICAL COMPONENT OF GROUND MOTION (Rock sites)

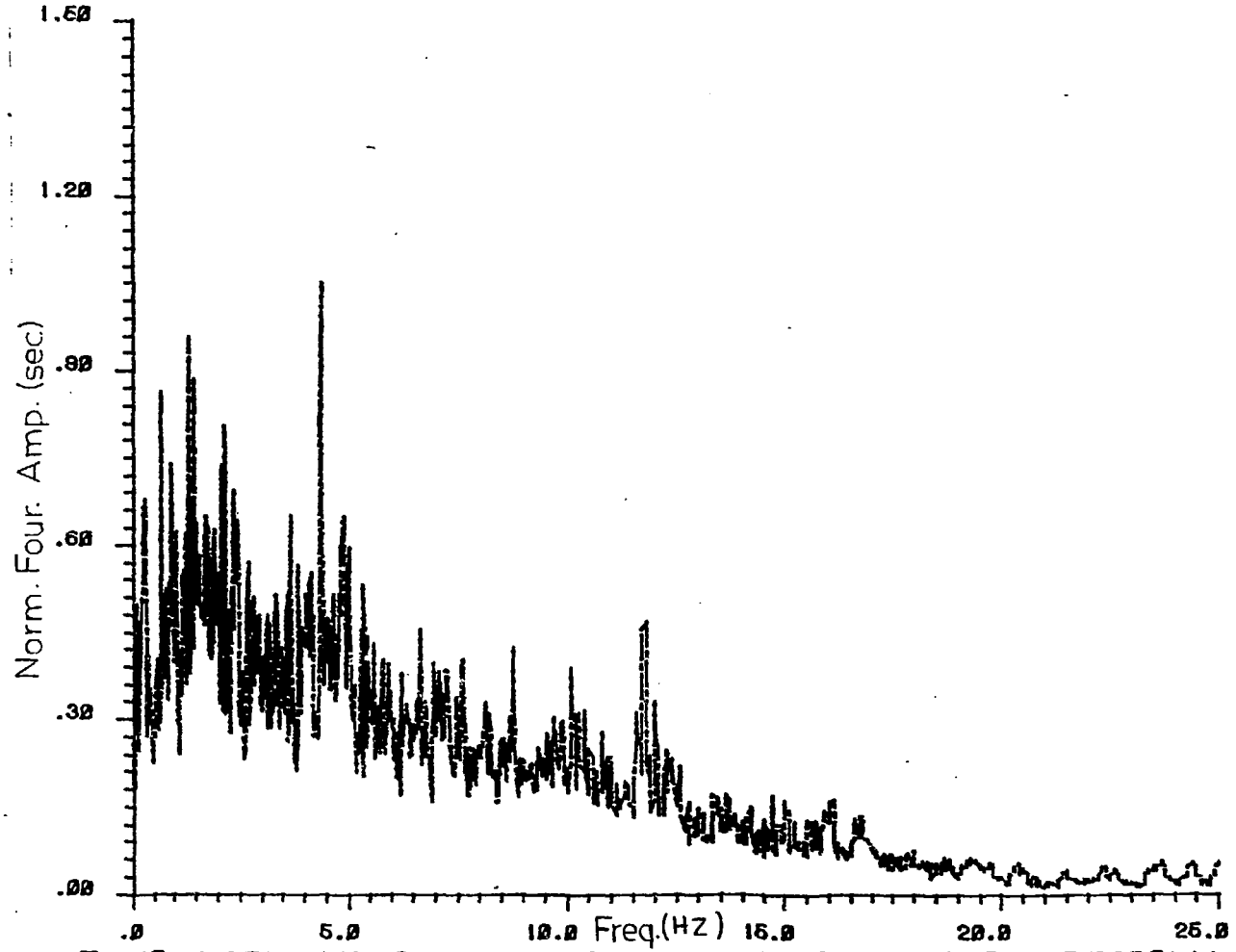

Fig.17: NORMALISED ENVELOPING FOURIER AMPLITUDE SPECTRUM FOR VERTICAL COMPONENT OF GROUND MOTION (Rock sites)

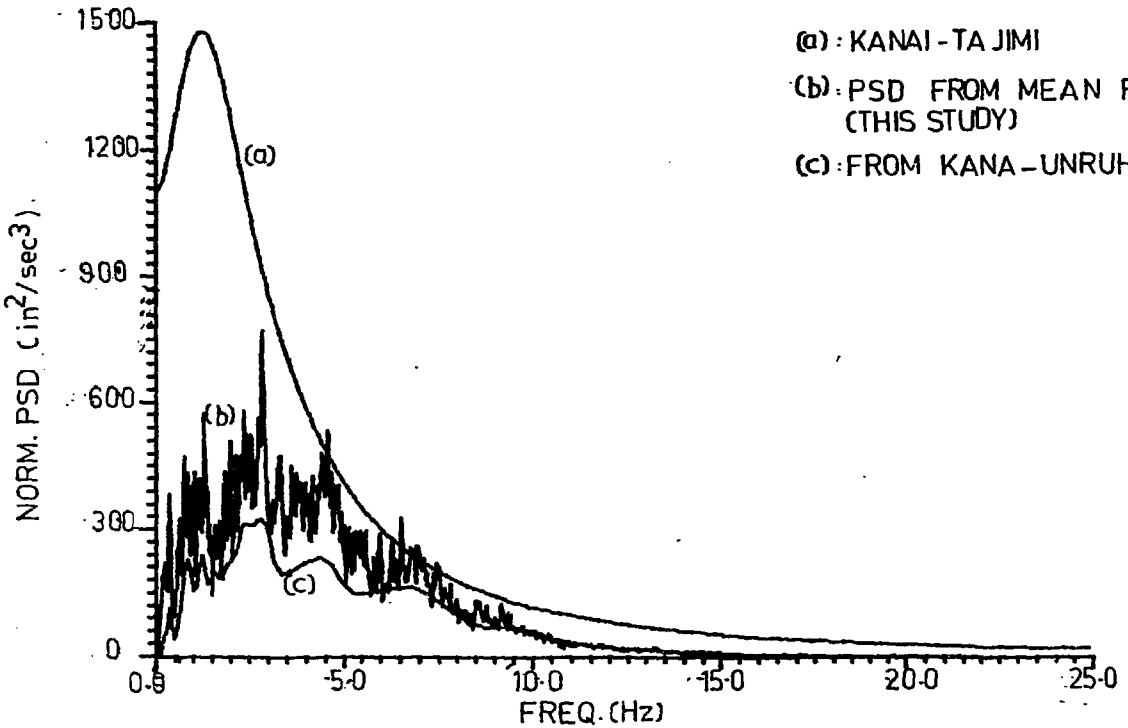

Fig. 18 : COMPARISON OF PSDFs OF HORIZONTAL GROUND MOTION

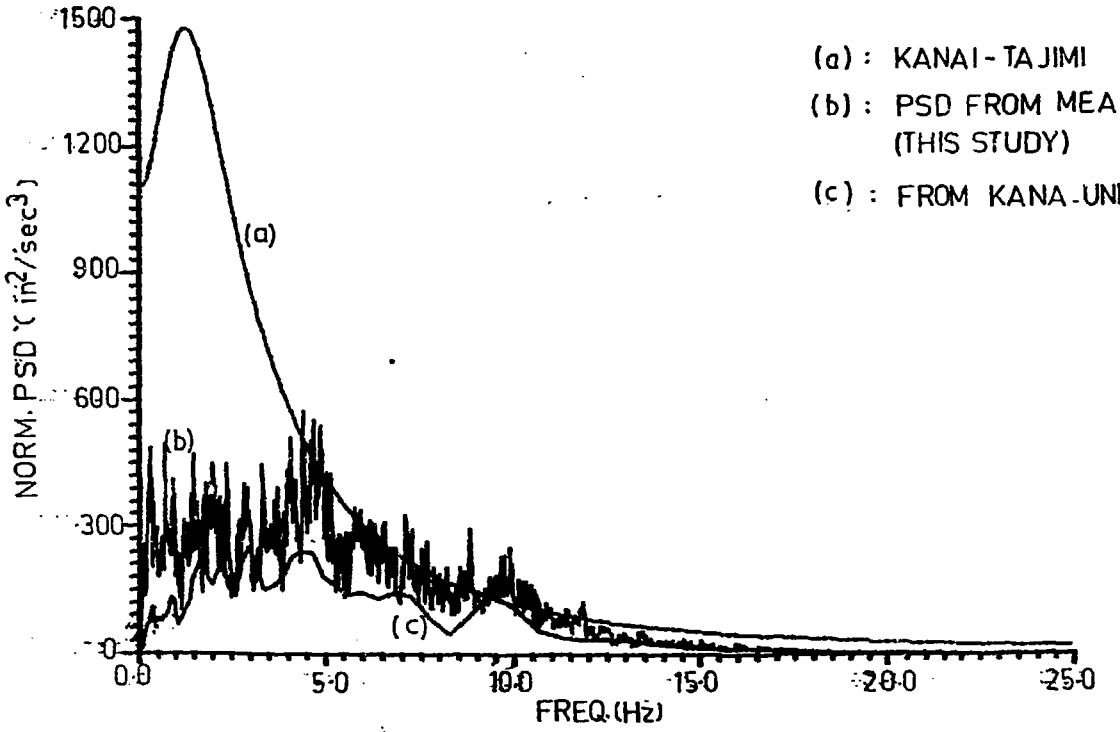

Fig.19: COMPARISON OF PSDFs OF VERTICAL GROUND MOTION

APPENDIX

A RECURSIVE ALGORITHM FOR EVALUATION OF DISCRETE FOURIER TRANSFORM

$$X_k = x(k\Delta f) = \Delta t \sum_{i=0}^{N-1} x_i \, e^{-\frac{j 2\pi i k}{N}} \qquad k = 0,1,2 \ldots\ldots N-1$$

$$= c_k - j q_k \quad \text{(say)} \qquad \ldots \text{(A-1)}$$

Then $$c_k = \Delta t \sum_{i=0}^{N-1} x_i \cos\frac{2\pi i k}{N} = \Delta t \sum_{i=0}^{N-1} x_i \cos(ai) \qquad \ldots \text{(A-2)}$$

$$q_k = \Delta t \sum_{i=0}^{N-1} x_i \sin\frac{2\pi i k}{N} = \Delta t \sum_{i=0}^{N-1} x_i \sin(ai) \qquad \ldots \text{(A-3)}$$

$$a = \frac{2\pi k}{N}$$

Let us consider the following trigonometric identities

$$\sin\left[(M-1)a\right] = \sin(Ma)\cos a - \cos(Ma)\sin a$$

$$\sin\left[(M+1)a\right] = \sin(Ma)\cos a + \cos(Ma)\sin a$$

Hence $$\sin\left[(M-1)a\right] + \sin\left[(M+1)a\right] = 2\sin(Ma)\cos a$$

or $$\sin\left[(M+1)a\right] = 2\cos a \sin(Ma) - \sin\left[(M-1)a\right] \qquad \ldots \text{(A-4)}$$

Similarly,

$$\cos\left[(M+1)a\right] = 2\cos a \cdot \cos(Ma) - \cos\left[(M-1)a\right] \qquad \ldots \text{(A-5)}$$

From equations (A.2) and (A.5) we have,

$$\frac{C_k}{\Delta t} = \sum_{i=0}^{N-2} x_i \cos(ai) + U_1 . \cos\left[(N-1)a\right]$$

$$\frac{C_k}{\Delta t} = \sum_{i=0}^{N-2} x_i \cos(ai) + x_{N-1}\left[2\cos a \cos\left[(N-2)a\right] - \cos(N-3)a\right]$$

$$= \sum_{i=0}^{N-3} x_i \cos(ai) + (x_{N-2} + 2\cos a\, x_{N-1}) \cos\left[(N-2)a\right]$$

$$- x_{N-1} \cos\left[(N-3)a\right]$$

$$= \sum_{i=0}^{N-4} x_i \cos(ai) + (x_{N-3} - x_{N-1}) \cos\left[(N-3)a\right]$$

$$+ (x_{N-2} + 2\cos a x_{N-1}) \cos\left[(N-2)a\right]$$

$$= \sum_{i=0}^{N-4} x_i \cos(ai) + (x_{N-3} - U_1) \cos\left[(N-3)a\right] + U_2 \cos\left[(N-2)a\right]$$

$$= \sum_{i=0}^{N-5} x_i \cos(ai) + x_{N-4} \cos\left[(N-4)a\right] + (x_{N-3} - x_{N-1}) . \cos\left[(N-3)a\right]$$

$$+ U_2 . \left[2\cos a \cos\left[(N-3)a\right] - \cos\left[(N-4)a\right]\right]$$

$$= \sum_{i=0}^{N-5} x_i \cos(ai) + (x_{N-4} - U_2) \cos\left[(N-4)a\right] + (x_{N-3} - x_{N-1} + 2U_2 \cos a) \cos(N-3)a$$

$$= \sum_{i=0}^{N-5} x_i \cos(ai) + (x_{N-4} - U_2) \cos\left[(N-4)a\right]$$

$$+ U_3 . \cos(N-3)a \qquad \ldots \quad (A-6)$$

Continuing in the same fashion equation, (A.6), after several simplications, will reduce to

$$\begin{aligned}\frac{C_k}{\Delta t} &= X_0 + (X_1 - U_{N-3}) \cos a + U_{N-2} \cos 2a \\ &= X_0 + (X_1 - U_{N-3}) \cos a + U_{N-2} (2\cos^2 a - 1) \\ &= X_0 + (X_1 + 2\cos a \cdot U_{N-2} - U_{N-3}) \cos a - U_{N-2} \\ &= X_0 + U_{N-1} \cos a - U_{N-2}\end{aligned} \qquad \ldots \quad (A\text{-}7)$$

where,

$$U_0 = 0 \qquad \ldots \quad (A\text{-}8)$$

$$U_1 = X_{N-1} \qquad \ldots \quad (A\text{-}9)$$

$$U_i = 2 \cos a \, U_{i-1} - U_{i-2} + X_{N-i}$$

$$i = 2, 3, \ldots N-1 \qquad \ldots \quad (A\text{-}10)$$

$$\begin{aligned}\frac{Q_k}{\Delta t} &= \sum_{i=0}^{N-1} x_i \sin(ai) \\ &= \sum_{i=0}^{N-2} x_i \sin(ai) + U_1 \sin[(N-1)a] \\ &= \sum_{i=0}^{N-2} x_i \sin(ai) + U_1 [2\cos a \sin[(N-2)a] - \sin[(N-3)a]] \\ &= \sum_{i=0}^{N-4} x_i \sin(ai) + [U_1 2\cos a + X_{N-2}] \sin[(N-2)a] \\ &\qquad + [X_{N-3} - U_1] \sin(N-3)a \\ &= \sum_{i=0}^{N-4} x_i \sin(ai) + [X_{N-3} - U_1] \sin[(N-3)a] + U_2 \sin[(N-2)a]\end{aligned} \qquad \ldots \quad (A\text{-}11)$$

Continuing in the same fashion, we have, after several simplifications

$$\frac{Qk}{\Delta t} = X_0 \cdot \sin(a \cdot 0) + (X_1 - U_{N-3}) \sin a + U_{N-2} \sin 2a$$

$$= (X_1 - U_{N-3}) \sin a + U_{N-2} \cdot 2 \sin a \cdot \cos a$$

$$= (X_1 + 2 \cos a \, U_{N-2} - U_{N-3}) \sin a$$

$$= U_{N-1} \sin a \qquad \ldots \quad (A\text{-}12)$$

Published by : M. R. Balakrishnan Head, Library & Information Services
Bhabha Atomic Research Centre Bombay 400 085